SLAC-PUB-95-6897
LBL-37250
May 1995

High-Power RF Window and Coupler Development for the PEP-II B Factory*

M. Neubauer, K. Fant, J. Hodgson, J. Judkins, H. Schwarz
Stanford Linear Accelerator Center, Stanford University, Stanford, CA 94309, USA
R.A. Rimmer,
Lawrence Berkeley Laboratory, 1 Cyclotron Road, Berkeley, CA 94720, USA

Abstract

We describe the fabrication and testing of the RF windows designed to transmit power to the PEP-II 476 MHz cavities. Design choices to maximize the reliability of the window are discussed. Fabrication technologies for the window are described and finite-element analysis of the assembly process is presented. Conditioning and high-power testing of the window are discussed. Design of the coupler assembly including the integration of the window and other components is reported.

1. INTRODUCTION

The RF design of a self-matched RF window using a 10 inch (254 mm) alumina disk in a WR2100 size waveguide is described in an earlier paper [1]. This paper describes the mechanical realization and initial power tests of the window design. To counteract tensile stress on the perimeter of the disk when heated by RF fields, a stainless steel rings is shrunk onto the ceramic during the brazing process. The stainless steel ring puts the ceramic disk in compression and thus results in a rugged window design capable of handling the 500 kW of RF power. To remove heat from the window, a cooling channel is included in the stainless steel ring. We describe the modeling and construction details of the brazing operation. The post-braze machining steps by which the window frequency and match are tuned to the desired values are also described. A knife-edge seal with a copper gasket was used to make a vacuum joint. To reduce multipactor each window is coated with titanium nitride. Two windows, back-to-back, are assembled onto a waveguide test chamber built to be evacuated and operated with up to 500 kW throughput power into a matched load. During the tests, calorimetric measurements were made and total power loss in the window and iris were calculated. Power loss and temperature measurements correlated well with ANSYS and MAFIA calculations.

2. WINDOW CONSTRUCTION DETAILS

2.1 Compression concept.

The challenge of the braze of a stainless steel compression ring to the ceramic disk is in the difference of expansion coefficients which makes the braze gap between the ceramic and the stainless steel ring widen as the window is heated to braze temperature. A molybdenum keeper ring with an expansion coefficient less than that of the ceramic and stainless steel is used to shrink fit the stainless steel ring (Fig. 1) onto the ceramic so that the braze gap is just right at the braze temperature.

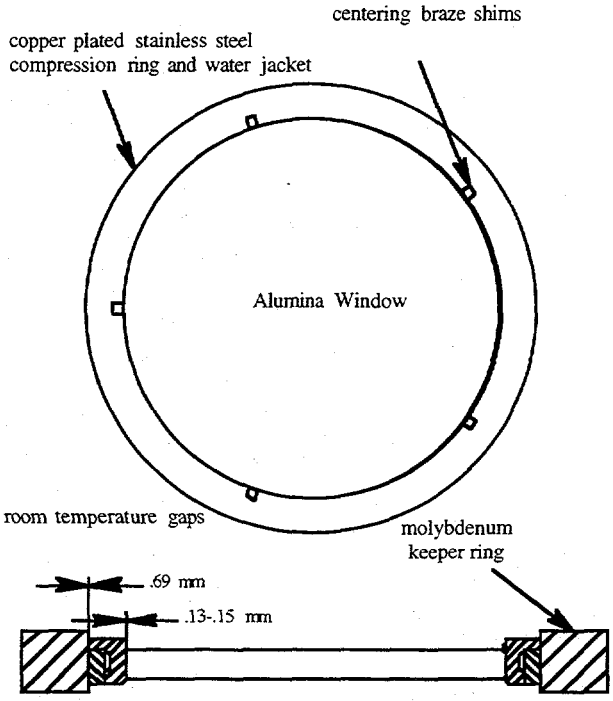

Figure1. Braze fixture details: centering shims, gaps at room temperature.

2.2 Braze modeling and results.

ANSYS modeling, 1/3 scale braze tests, and full size braze tests were required to learn the critical parameters required to control the braze gap, volume of braze material, and the size of the fillet. The gap between the metallized alumina ceramic and the copper buffer layer on the inside diameter of the stainless steel compression ring we found to require a dimension of .075±.004 mm at braze temperature. Too small of a gap would not allow full flow of the braze alloy along the 18.3 mm edge of the window and cause leaks. Too large of a gap would not allow the braze to fully bridge the gap and possibly cause stress concentrators and/or leaks. Because of the large size and mass of the various components, a technique was also required to keep the braze gap uniform around the perimeter of the window during the heating to brazing temperature (1050°C). This was accomplished with braze

*Work supported by Department of Energy contracts
DE-AC03-76SF00515 (SLAC)
DE-AC03-76SF00098 (LBL)

Presented at the 16th IEEE Particle Accelerator Conference (PAC 95) and International Conference on High Energy Accelerators, Dallas, Texas, May 1-5, 1995

shims of the braze alloy as shown in Figure 1. which maintained concentricity until they melted and were absorbed into the braze joint.

For the optimum gap at brazing temperature, the room temperature clearances required between the molybdenum keeper ring, stainless steel compression ring and alumina ceramic, were determined by ANSYS analysis, 1/3 scale models and finally by full-size trials. The required gaps are shown in Figure 1. These critical gaps were achieved by measuring the inside diameter of the molybdenum keeper ring and the outside diameter of the nickel plated, metallized alumina ceramic, to accuracies of .0025mm. The inside and outside diameter of the copper plated stainless steel compression ring is then custom machined to achieve the critical room temperature gap dimensions.

A significant factor in the consistency of the braze gap at 1050°C, was discovered to be the frictional contact between the molybdenum keeper ring and the stainless steel compression ring. The gap between the stainless steel compression ring and the inside diameter of the molybdenum keeper ring closes to zero at approximately 500°C. During the continued rise in temperature, the stainless steel ring yields in compression modified by frictional forces and the degree of sticking. The contact elements in the ANSYS library allowed us to model the influence of friction. A titanium nitride coating on the inside of the keeper ring, and a "green-fired" or chrome-oxide coated outside surface on the compression ring were the surface treatments which produced the most reliable and repeatable frictional forces with minimized sticking.

After all the control variables were optimized we produced three prototype windows which were all leak-tight and compressed. Figure 2, shows one of the post-machined windows with knife-edge seal.

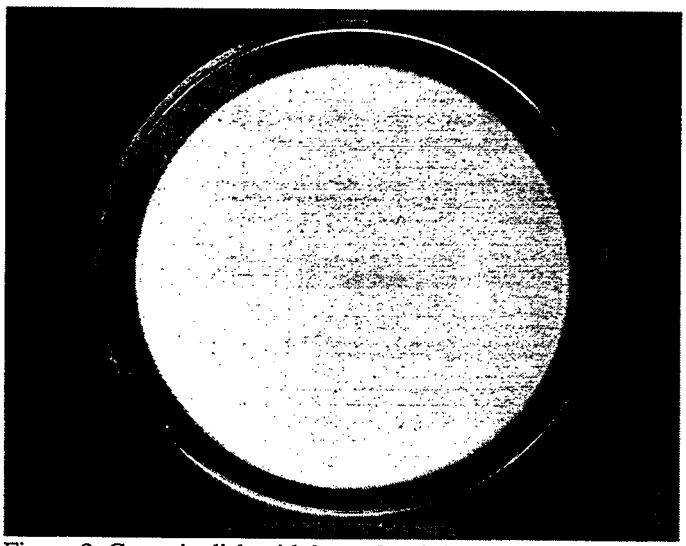

Figure 2. Ceramic disk with brazed stainless steel compression ring and post-machined knife-edge seal.

2.3 Fine-tuning of the match.

After brazing the height of the compression ring is machined back to create an iris length which achieves the desired match frequency of the window. This also eliminates any distortion from the brazing process. The sensitivity of this machining step agreed well with the HFSS calculations and was measured to be 1.4 MHz/mm. The outside diameter of the stainless steel ring is also made true for the best match possible. The final result of these machining operations are shown in Figure 3, with a minimum VSWR of 1.01

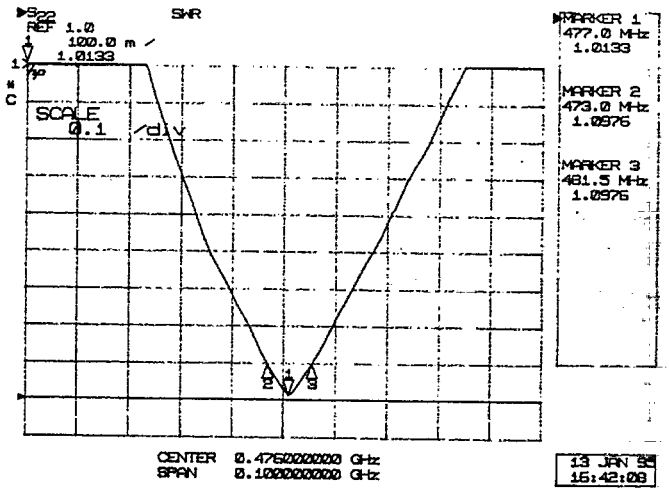

Figure 3. Cold Test match of a brazed and post machined Self-Matched window measured in the coupler transition. (The center frequency will shift down to 476 MHz when the knife-edge vacuum seal is fully compressed.)

2.4. Vacuum Seal.

A knife-edge seal using a copper gasket was chosen. The knife-edge is cut as part of the post machining of the stainless steel compression ring. The other half of the knife-edge vacuum seal is the stainless steel flange of the 16" x 9" waveguide. A picture of this seal assembly is shown in Figure 4.

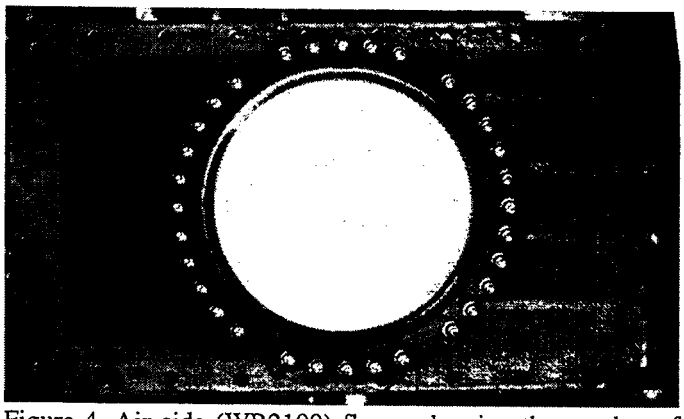

Figure 4. Air side (WR2100) flange showing the number of bolts required to provide the necessary force to make the vacuum seal.

3. HIGH POWER TESTING

3.1. Test Chamber.

The vacuum test chamber for the back-to-back window test is shown in Figure 5. The chamber was designed with viewports to observe the window surfaces. Photo-multiplier arc-detectors sensitive to UV and visible light were also included in a position to observe the high-field triple junction portion of the window. An Infrared Imaging camera was used to record window temperatures from the air side. Flow meters and thermistors were used to calculate total power loss in the individual windows.

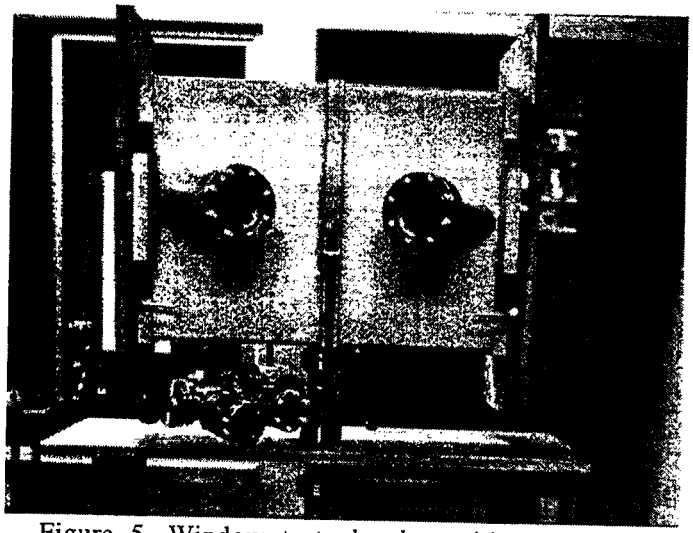

Figure 5. Window test chamber with two windows assembled.

3.2. Preliminary Results of RF Power Tests.

The goal is to process the assembly of two back-to-back windows with vacuum in between to 500 kW power transmission. During initial processing we were able to run CW power levels up to 400 kW for several minutes limited by outgassing as the ceramic heated up. Under continuous operation we were able to reach 270 kW of CW power limited by additional heating of the ceramic due to multipactor. The multipactor shows itself as a strong purple glow on the ceramic. It does not seem to process away with CW or pulsed processing. As a next step we will increase the titanium nitride coating thickness and retest.

3.3. Ohmic-loss Measurement.

To check the ohmic loss behavior of the test windows, the test chamber was backfilled with dry nitrogen and tested up to 500 kW of CW power. With the infrared imaging camera, we measured the thermal profile during warm up and at steady state. The iso-therms in the temperature profile had a tendency to be oval shaped with the highest temperatures on the perimeter in the high current region. The profiles are shown in Figure 6. These results agree well with our predictions from ANSYS and MAFIA calculations at this power level. We also used MAFIA to make the following calculations at 500 kW of CW power: surface wall currents in the metallizing and nickel plating on the ceramic perimeter produce 150 watts, dielectric losses in the ceramic produce 157 watts, and iris wall losses produced 71 watts. These loss calculations totaled 378 watts. At 500 kW in air, we found excellent agreement with 327 watts measured on one window and 350 watts on the other.

4. COUPLER GEOMETRY

The coupler geometry designed for the RF cavity places the window around a 90° E-bend, away from direct line-of-sight of the beam. The 16"x9" (406x23 mm) rectangular waveguide size was chosen to place the window in a cavity detuned short position to limit the voltge excursions during RF transients [2].

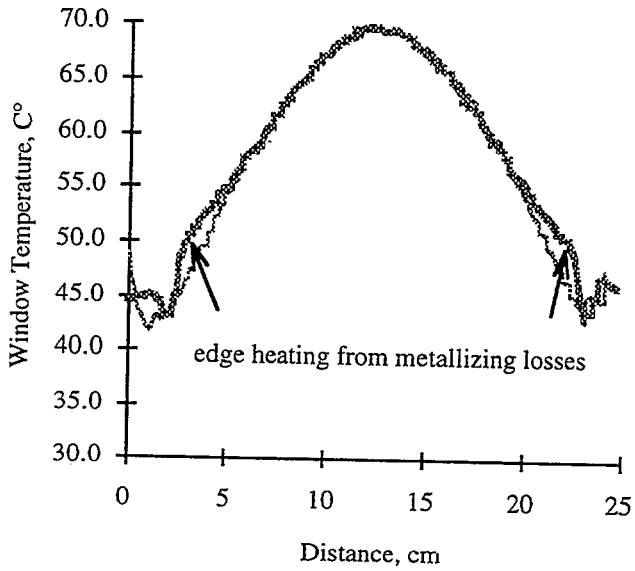

Figure 6. Temperature profile across the window with 500 kW incident power (thin line parallel to E field, thick line orthogonal to E-field)

5. CONCLUSIONS

The manufacturing method for producing pre-stressed windows is complete. RF Power tests are encouraging. The anti-multipactor coating requires further optimization. The ohmic-loss measurements agree with the calculations.

6. ACKNOWLEDGMENTS

We would like to thank Alan Hill for his design and configuration of the automated High Power Test data collection system.

7. REFERENCES

[1] M. Neubauer et al, "High-Power RF Window Design for the PEP-II B Factory, "Proc EPAC 94, June 27-July 1 1994, London

[2] H. Schwarz et al, "RF System Design for the PEP-II B Factory," Proc EPAC 94, June 27-July 1 1994, London

DISCLAIMER